Structural, electronic and mechanical properties of TiNbVZrHf alloy

Lebogang Motsomone[1*], *Ramogohlo* Diale[2], *Phuti* Ngoepe[1] and *Hasani* Chauke[1]
[1]Materials Modelling Centre, University of Limpopo, Private Bag X 1106, Sovenga, 0727, South Africa
[2]Advanced Materials Division, MINTEK, Private bag X 3015, Randburg, 2125, South Africa

Abstract. High entropy alloys (HEAs) are identified as essential materials for enhancing hydrogen storage applications. However, hydrogen storage processes and the material used are still a challenge, since no single material meets all the requirements. In this study, density functional theory technique is employed to aid in the design of TiNbVZrHf alloy with potential applications for hydrogen storage by examining their structural and mechanical properties. The calculated lattice parameters agree well with the experimental data, within 2%. The band structure showed that the alloy conducts electricity. Additionally, TiNbVZrHf was found that to be mechanically stable and has ductile behaviour. The findings will contribute to the development of HEAs as alternative materials for hydrogen storage.

1 Introduction

High entropy alloys (HEAs) are alloys that contains a high concentration of multi-principal elements [1]. Unlike traditional alloys, they do not relay on a single main elements. They are created by the combination of five or more main elements in equalmolar proportions or nearly equimolar ratios [2]. These alloys can form solid solutions, with structures such as body-centered cubic (BCC), face-centered cubic (FCC), and hexagonal close-packed (HCP) types [3]. The high configurational entropy of HEAs contributes to their exceptional strength, ductility, and corrosion resistance, which makes them particularly well-suited for use in demanding environments [4]. For example, HEAs have demonstrated unique characteristics that are particularly advantageous in high-temperature applications in gas turbines, rocket nozzles, and nuclear construction [5, 6]. Low-density refractory HEAs, in particular, are well-suited for the aerospace sector, where lightweight materials that can endure extreme temperatures are critical [5]. Furthermore, HEAs exhibit superior cryogenic properties, making them suitable for applications such as rocket casings, piping, and equipment designed to handle liquid oxygen or nitrogen [7].

HEAs show significant potential for hydrogen storage applications due to their remarkable ability to store hydrogen as hydrides in a range of hydrogen-to-metal ratios [8]. These alloys exhibit exceptional hydrogen storage properties, including high storage capacity, rapid hydrogen absorption and desorption at moderate temperatures and pressures [9]. According to the recent research, alloys originating from the Ti-V-Nb system might be

* Corresponding author: lmotsomone@gmail.com

promising contenders to store hydrogen. For example, TiVNbCr [10], exhibited a remarkable capacity for reversible hydrogen storage at room temperature and moderate pressures (1.96% wt%) without requiring any activation process. Furthermore, to create an equimolar TiZrNbMoV alloy, Kunce et al. [11] used the additive manufacturing process known as laser-engineered net shaping (LENS). This material demonstrated a hydrogen absorption capacity of 1.79 hydrogen atoms per metal atom (H/M), corresponding to 2.3 wt.%.

However, there are several challenges associated with the materials and methods currently used for hydrogen storage. One of the primary issues is the limited capacity of these alloys to store hydrogen efficiently. Existing methods often require high temperatures and pressures, which can be both costly and impractical for widespread adoption [12]. Additionally, much research has focused on hydrogen storage capacity, However, the understanding of the structural properties of materials before hydrogenation remain insufficiently understood. This lack of knowledge makes it difficult to predict and improve hydrogen storage performance. Further investigation into the structures of pre-hydrogenation materials is necessary to enhance the design and efficiency of hydrogen storage systems.

Hence, the purpose of the study is to is to use computational techniques, particularly density functional theory (DFT), were utilized to investigate structural and mechanical properties of the TiNbVZrHf high entropy alloy. The examination of structural properties such as phase formation is a critical consideration, as materials must possess the ability to develop stable phases with hydrogen. This capability is particularly important, as hydrogen storage materials depend on phase transitions to efficiently absorb and release hydrogen. Additionally, a comprehensive understanding of the mechanical properties of materials, including ductility and toughness, is essential in the design of alloys that resist embrittlement, thereby enhancing their durability and reliability.

2 Methodology

The calculations are performed using a first-principles method that is based on the DFT coded within the Vienna ab initio simulation package (VASP) code [13]. A generalized gradient approximation (GGA) [14] of Perdew-Burke-Ernzerhof (PBE) [15] addressed the exchange-correlation effect. Extensive electron interactions have been described using the projection-enhanced wave method (PAW) [16, 17]. for Ti, V, Nb, Zr and Hf, the extranuclear electrons were selected as $3d^24s^2$, $3d^34s^2$, $4p^64d^45s^1$, $4d^25s^2$ and $6d^246s^2$, respectively. Monkhorst-Pack grids were used to integrate over Brillouin zone sampling to ensure highly converged results. The total energy of the structures was converged using a k-point mesh of 5x5x5 and a kinetic energy cutoff of 500 eV. When calculating elastic properties, 0.006 strain was chosen for the lattice deformation. The phase formation parameters of the alloy were predicted using the High-Entropy Alloys Predicting Software (HEAPS) [18].

3 Results and discussion

3.1 Structural properties

Figure 1(a) presents a detailed depiction of the crystal structure of a single-site TiNbVZrHf high-entropy alloy, which is represented by a supercell with dimensions of 2 x 5 x 5. This supercell comprises a total of 100 atoms, with each of the five constituent elements, titanium (Ti), niobium (Nb), vanadium (V), zirconium (Zr), and hafnium (Hf), each contributing 20 atoms. The arrangement of these elements results in a solid solution, characterized by randomly distributed atomic positions. The X-ray diffraction (XRD) (figure 1(b)) reveals that the TiNbVZrHf alloy crystallizes in a body-centred cubic (BCC) configuration, which

belongs to the Im3m space group (No. 229). The results indicated that the calculated lattice parameter (a = 3.306 Å) and the experimental value (a = 3.3659 Å [19]), are in good agreement, to within 2%. The slight discrepancy of less than 2% between these values underscores the reliability of the computational methods used and suggests that the theoretical model effectively captures the essential characteristics of the alloy structure.

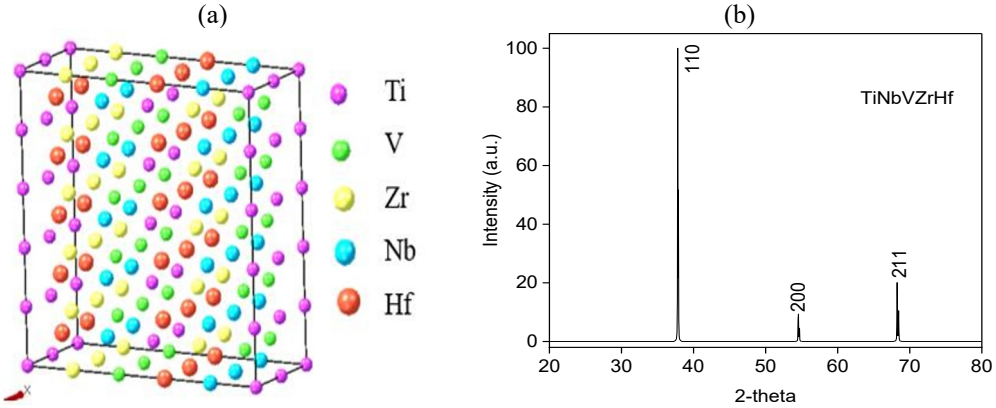

Fig. 1. (a) Atomic arrangement and (b) X-ray diffraction (XRD) Pattern of TiNbVZrHf high entropy alloy.

3.2 Thermodynamic phase formation

The enthalpy (ΔH_{mix}) and entropy (ΔS_{mix}) of mixing, the atomic size difference (δ), ration of entropy and enthalpy of mixing (Ω) and valence electron concentration (VEC) are key parameters that can be used to predict whether the alloy can form a solid solution phase.

Table 1. The calculated ΔH_{mix} and ΔS_{mix}, the δ, Ω and VEC of TiNbVZrHf alloy.

Parameter	Formular	TiNbVZrHf
ΔH_{mix} (KJ/mol)	$\Delta H_{mix} = \sum_{i=1,i\neq j}^{N} 4\Delta H_{AB}^{mix} c_i c_j$	0.8
ΔS_{mix}(J/Kmol)	$\Delta S_{mix} = RlnN$	13.4
δ (%)	$\delta = \sqrt{\sum_{i=1}^{N} c_i(1 - r_i/(\sum_{i=1}^{N} c_i r_i))^2}$	7.1
Ω(T)	$\Omega = T_{mix}\Delta S_{mix}/\lvert\Delta H_{mix}\rvert$	38.5
VEC	$VEC = \sum C_i(VEC_i)$	4.4

$c_i c_j$ is the atomic percentage of the i-th (j-th) component. r_i is the atomic radius, R is the gas constant and N the number of microstates or distinguishable configuration and T_{mix} = 2302 and is the mixing temperature of the alloy

A solid solution phase in high-entropy alloys provides structural simplicity, efficient diffusion pathways, thermodynamic flexibility, and mechanical stability, which are all

essential for effective and reversible hydrogen storage. Table 1 presents the thermophysical parameters proposed for predicting phase formation.

The solid solution is considered thermodynamically stable due to a high entropy of mixing (ΔS_{mix}), which can occur if the enthalpy of mixing (ΔH_{mix}) is low. Zhang et al. (2008) [20] proposed that high entropy alloys typically form solid solution phases when the mixing enthalpy is within the range of -10 KJ/mol $< \Delta H_{mix} < 5$ KJ/mol, as long as the mixing entropy is between 12 J/Kmol $< \Delta S_{mix} <$17 J/Kmol, and the atomic radius difference (δ) is less than 6.5% [19]. Additionally, Yang et al. (2014) [21] introduced the parameter Ω to illustrate the thermodynamic stability of multi-principal element disordered solid solutions at room temperature, indicating that the solid solution is relatively stable when Ω (T) > 1. Our results show that ΔHmix is low (0.8 kJ/mol), leading to a high entropy of 13.3, and Ω (T) > 1, thereby satisfying these stability conditions. This suggests that the structure is thermodynamically stable and capable of forming a solid solution.

However, we found that $\delta > 6.5\%$, which indicate that the intermetallic compounds may form rather than a solid solution. This may be results from the significant size difference between atoms like V and Zr or Hf, which causes the lattice strain and drives the system towards intermetallic formation to reduce energy. Guo et al. (2011) [22] introduced the Valence Electron Concentration (VEC) criterion, which suggests that FCC phases exhibit greater stability when VEC exceeds 8.6, BCC are more stable when VEC is below 6.87 [23, 24]. Our results indicate that the structure adopts a BCC solid solution phase as VEC is 4.4. This indicates that the alloy's crystal lattice will accommodates hydrogen atoms within its interstitial sites with minimal structural disruption.

3.3 Electronic properties

The band structure calculations were conducted to gain a better understanding of the electronic properties of TiNbVZrHf alloy. This approach helps determine how easily an electron can be excited from the valence band (where electrons generally exist) to the conduction band (where electrons can travel freely and enhance electrical conductivity). The analysis reveals the distribution of energy bands. Figure 2 presents the band structure of TiNbVZrHf along the Z, G, X, P, N and G Brillouin zone directions. From this figure, no band gap at the Fermi level was found. The results suggests that TiNbVZrHf is a conductor, which allows the current to flow when energy is supplied, such as through heat. Additionally, this observation suggests that electrons are available to participate in both the formation and dissociation of hydrogen bonds.

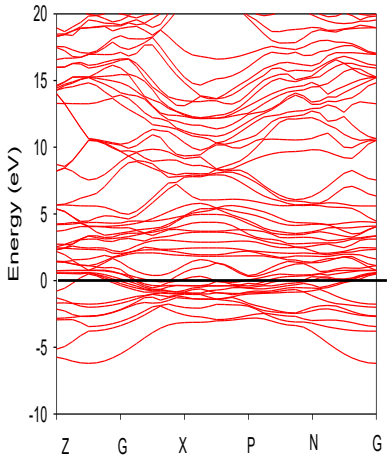

Fig. 2. The calculated electronic band structure for TiNbVZrHf structure.

Figure 3 shows the total density of states (tDOS) and the partial density of states (pDOS) for TiNbVZrHf alloy. From the graph the black dashed line represents the fermi energy, which is used as the zero of the energy scale. The tDOS has peaks at certain energy values, which indicate specific electronic states (s, p and d states). Meanwhile, the pDOS gives insights into how different atomic orbitals contribute to the overall density of states. It can be noted that there are states observed at the Fermi level (E_F), which indicates that the structure shows a metallic behaviour. Furthermore, there was no pseudo-gap was observed at the E_f which indicates that the structure is electronically unstable. The pDOS shows a very broad peak in the valence band contribution concentrated at -8 eV, which consists mainly of d-orbital. Then follows by the peak contribution at 0 eV (Fermi), which also consists mainly of d- orbital corresponding to a peak in the tDOS. The lower peak of the conduction band is dominated by the d-orbital, ranging around 2 eV to 7 eV. All the upper peaks ranging in the conduction band at 8 eV to 20 eV are occupied by the s - and p- orbitals.

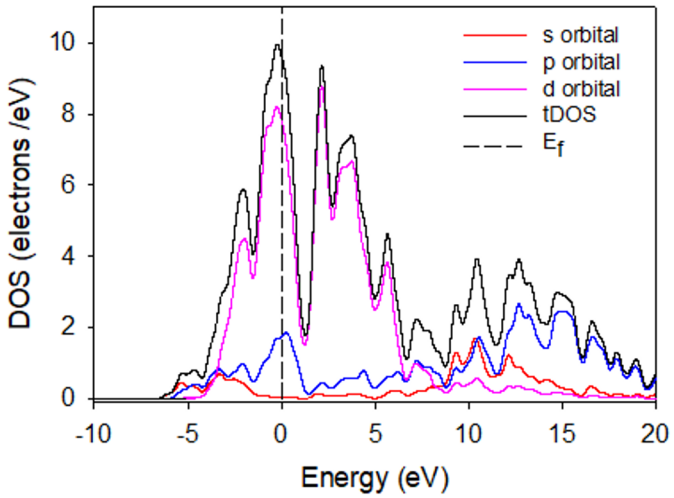

Fig. 3. The calculated total and partial density of state for TiNbVZrHf alloy.

3.4 Elastic properties

The calculated elastic properties of TiNbVZrHf high entropy alloy are shown in Table 2. One of the most crucial physical characteristics of materials is their elasticity. Understanding elastic properties is crucial for experimental mechanics as well as structural design. [25]. The elastic constant serves as an indicator of a material's mechanical stability, with varying structural orientations imposing distinct criteria. The stability criterion for the elastic constants must be fulfilled for the structure to be classified as stable. In the case of a cubic system, the number of independent elastic moduli is reduced from 39 to 9 as $c_{ij} = c_{ji}$ and there being strong symmetry in the two lattice [26]. The mechanical stability condition for a cubic system can be defined by [27]:

$$c_{44}>0;\ \ c_{11}>c_{12} \text{ and } c_{11}+2c_{12}>0 \qquad (1)$$

The results indicate that TiNbVZrHf alloy satisfies the cubic stability criteria, since c_{ij} are positive. Therefore, the structure is mechanically stable. This also indicates that the alloy can withstand multiple cycles of hydrogen absorption and release without deteriorating.

The elastic moduli such as bulk (B), shear (G), and Young ‘s modulus (E) are also determined. The bulk modulus assesses how a solid resists changes in volume and provides an estimate of the elastic behaviour of the material when subjected to hydrostatic pressure. The shear modulus characterises a material's ability to resist deformation. Lastly, Young’s modulus describes the relative stiffness of a material. The structure also has high values of B, G, and E modulus, indicating that it can bear large stress and deformation without failure. This suggest that the alloy can accommodate hydrogen without degrading. The ductility of the alloy was also investigated, this was determined using the Pugh and Poisson ratios. Pugh proposed the value of B/G is related to the material's malleability and brittleness. In particular, a high B/G value indicate malleability, whereas a low value is suggested to indicate brittleness. Moreover, the value of 1.75 [28] is a critical point that distinguishes between ductile and brittle materials. Poisson’s ratio can also be rewritten based on the bulk and shear modulus as follows [29]:

$$\sigma = \frac{3B-2G}{2(3B+G)} \ , \tag{2}$$

To obtain ductility, the value must be greater than 0.26 [30]. The data revealed that the structures demonstrate ductility as their values are more than 1.75 and 0.26 for B/G and σ ratios, respectively. This suggest that TiNbVZrHf alloy is likely to survive the stress caused by hydrogen absorption/desorption without cracking.

Table 2. Elastic properties of TiNbVZrHf high entropy alloy.

Elastic Properties	Alloy: TiNbVZrHf
Elastic constant (c_{ij})	
C_{11}	320.16
C_{12}	219.41
C_{44}	44.08
Elastic Moduli (GPa)	
Bulk modulus (B)	266.78
Shear modulus (G)	39.92
Young’s modules (E)	114.06
Ductility	
Pugh ratio (B/G)	6.682
Poisson ratio (σ)	0.428

4 Conclusion

Using the first principle approach, we studied the structural and mechanical properties of TiNbVZrHf high entropy alloy. The lattice parameters matched the experimental results within 2%. The structure was found to form a solid solution phase with a BCC configuration, which this makes the structure a highly desirable material for various hydrogen storage application. Furthermore, results showed the alloy to be mechanically stable at room temperature. The pugh and poisson ratio indicated that the TiNbVZrHf high entropy alloy has a ductile behaviour. The results obtained indicated that TiNbVZrHf alloy is preferred for reversible absorption and desorption of hydrogen.

The work was conducted at the Materials Modelling Centre, University of Limpopo. The authors wish to acknowledge the Centre of High-Performance Computing (CHPC) for computational resources.

The work was supported by the Department of Science, Technology and Innovation (DTSI) through the Council for Scientific and Industrial Research (CSIR).

Data availability: Data reported in this paper is available upon request to the corresponding author.

References

1. L. Kong, B. Cheng, D. Wan, Y. Xue, A review on BCC-structured high-entropy alloys for hydrogen storage. Front Mater, **10**,1135864 (2023)
2. F Marques, M. Balcerzak, F. Winkelmann, G. Zepon, M. Felderhoff, Review and outlook on high-entropy alloys for hydrogen storage. Energy Environ. Sci., **14**, 5191-5227 (2021)
3. F Marques, H.C. Pinto, S.J.A. Figueroa, F. Winkelmann, M. Felderhoff, W.J. Botta, G. Zepon, Mg-containing multi-principal element alloys for hydrogen storage: A study of the MgTiNbCr0. 5Mn0. 5Ni0. 5 and Mg0. 68TiNbNi0. 55 compositions. Int. J. Hydrog. Energy, **45**, 19539-19552 (2020)
4. M. Dada, P. Popoola, N. Mathe, Recent advances of high entropy alloys for aerospace applications: A review. World J. Eng, **20,** 43-74 (2023)
5. Y.F. Ye, Q. Wang, J. Lu, C.T. Liu, Y. Yang, High-entropy alloy: challenges and prospects. Mater. Today, **19**, 349-362 (2016)
6. T.P. Yadav, A. Kumar, S.K. Verma, N.K. Mukhopadhyay, High-entropy alloys for solid hydrogen storage: potentials and prospects. Transactions of the Indian National Academy of Engin, **7**, 147-156 (2022)
7. O.N. Senkov, G.B. Wilks, J.M. Scott, D.B. Miracle, Mechanical properties of Nb25Mo25Ta25W25 and V20Nb20Mo20Ta20W20 refractory high entropy alloys. Intermetallics, **19**, 698-706 (2011).
8. R. Floriano, G. Zepon, K. Edalati, G.L. Fontana, A. Mohammadi, Z. Ma, H.W. Li, R.J. Contieri, Hydrogen storage properties of new A3B2-type TiZrNbCrFe high-entropy alloy. Int. J. Hydrog. Energy, **46,** 23757-23766 (2021)
9. J. Zhang, J. Hu, H. Xiao, H. Shen, L. Xie, G. Sun, X. Zu, A first-principles study of hydrogen desorption from high entropy alloy TiZrVMoNb hydride surface. Metals, **11**, 553 (2021)
10. B.H. Silva, C. Zlotea, Y. Champion, W.J. Botta, G. Zepon, Design of TiVNb-(Cr, Ni or Co) multicomponent alloys with the same valence electron concentration for hydrogen storage. J. Alloy. Compd, **865,** 158767 (2021)
11. J.F. Kunce, J.R. West, N.D. Browning, J.W. Stevenson, Laser engineered net shaping of TiZrNbMoV high entropy alloy for hydrogen storage. Int. J. Hydrog. Energy, **39**, 9904-9911(2014).
12. R. Floriano, G. Zepon, K. Edalati, G.L Fontana, A. Mohammadi, Z. Ma, H.W. Li, R.J. Contieri, Hydrogen storage in TiZrNbFeNi high entropy alloys, designed by thermodynamic calculations. Int. J. Hydrog. Energy, **45**, 33759-33770 (2020)
13. G. Kresse, J. Hafner, Ab initio molecular dynamics for liquid metals. Phys. Rev. B, **47**, 558 (1993)
14. J.P. Perdew, K.K. Burke, M. Ernzerhof, Generalized Gradient Approximation Made sample. Phys. Rev. Lett, **77**, 3865 (1996)
15. J.P. Perdew, W. Yue, Correlation hole of the spin-polarized electron gas, with exact small-wave-vector and high-density scaling. Phys. Rev. B, **24**, 13298 (1991)
16. G. Kresse, D. Joubert, From ultrasoft pseudopotentials to the projector augmented-wave method, Phys. Rev. B, **59**, 1758 (1999).
17. E. Kucukbenli, M. Monni, B.I. Adetunji, X. Ge, G.A. Adebayo, N. Marzari, S. De Gironcoli, A.D. Corso, Projector augmented-wave and all-electron calculations across

the periodic table: a comparison of structural and energetic properties comparison of structural and energetic properties, Phys. Rev. B, **90**, 20510 (2014).

18. P. Martin, C.E. Madrid-Cortes, C. Cáceres, N. Araya, C. Aguilar, J.M. Cabrera, HEAPS: A user-friendly tool for the design and exploration of high-entropy alloys based on semi-empirical parameters. Comput. Phys. Commun, **278,** 108398 (2022)
19. D. Karlsson, G. Ek, J. Cedervall, C. Zlotea, K.T. Møller, T.C. Hansen, J. Bednarcik, M. Paskevicius, M.H. Sørby, T.R. Jensen, U. Jansson, Structure and hydrogenation properties of a HfNbTiVZr high-entropy alloy. Inorg. Chem, **57**, 2103-2110 (2018).
20. Y. Zhang, T.T. Zuo, Z. Tang, M.C. Gao, K.A. Dahmen, P.K. Liaw, Z.P. Lu, Criteria for solid solution formation in high-entropy alloys, J. Mater. Sci. Technol, **24**, 1931-1935 (2008).
21. X. Yang, Y. Zhang, Prediction of high-entropy stabilized solid-solution in multi-component alloys, Mater. Chem. Phys, **132**, 233-238 (2014).
22. S. Guo, C. Ng, J. Lu, C.T. Liu, Effect of valence electron concentration on stability of fcc or bcc phase in high entropy alloys, J. Appl. Phys, **109**, 103505 (2011).
23. F. Yang, J. Wang, Y. Zhang, Z. Wu, Z. Zhang, F. Zhao, J. Huot, J.G. Novaković, N. Novaković, Recent progress on the development of high entropy alloys (HEAs) for solid hydrogen storage: A review. Int. J. Hydrog. Energy, **47**, 11236-11249 (2022)
24. M.M. Nygård, G. Ek, D. Karlsson, M.H. Sørby, M. Sahlberg, B.C. Hauback, Counting electrons-a new approach to tailor the hydrogen sorption properties of high-entropy alloys. Act. Mater, **175,** 121-129 (2019)
25. L. Pagnotta, Recent progress in identification methods for the elastic characterization of materials. Int. J. mech, **2**, 129-140 (2008)
26. P.S. Nnamchi, C.S. Obayi, Concept of Phase Transition Based on Elastic Systematics, (In Elasticity of Materials-Basic Principles and Design of Structures, IntechOpen, 2018)
27. M. J. Mehl and B. M. Klein, First-Principles Calculation of Elastic Properties, (Wiley and Sons Ltd, **1**, 195-210 1994)
28. S.F. Pugh, Relations between the elastic moduli and the plastic properties of polycrystalline pure metals, J. Sci, **367**, 823-843 (1954)
29. R. Hill, First-principles elastic constants for the hcp transition metals Fe, Co, and Re at high pressure. Proceedings of the Physical Society, **65,** 350 (1952)
30. G.N. Greaves, A.L. Greer, R.S. Lakes, T. Rouxel, Poissons Ratio and Modern Material. Nat. Mater, **10**, 823-837 (2011)